Coherent stimulated x-ray Raman spectroscopy: Attosecond extension of resonant inelastic x-ray Raman scattering

Upendra Harbola[1] and Shaul Mukamel[2]
[1]*Department of Chemistry and Biochemistry, University of California–San Diego, San Diego, California 92093-0340, USA*
[2]*Department of Chemistry, University of California–Irvine, Irvine, California 92697-2025, USA*
(Received 24 November 2008; published 11 February 2009)

Spontaneous and stimulated resonant inelastic x-ray Raman-scattering signals are calculated using the Keldysh-Schwinger closed-time path loop and expressed as overlaps of doorway and window electron-hole wave packets. These are recast in terms of the one-particle Green's functions and expansion coefficients of configuration-interaction singles for valence excitations, which can be obtained from standard electronic structure codes. Calculation for many-body states of ground and core-excited systems is avoided.

DOI: 10.1103/PhysRevB.79.085108 PACS number(s): 33.20.Rm, 42.65.Dr, 42.65.Re

I. INTRODUCTION

Resonant nonlinear spectroscopy in the x-ray regime may become possible by new bright ultrafast sources.[1–5] The theoretical formulation of nonlinear spectroscopy with attosecond x-ray pulses is of considerable interest.[6–9] The picosecond optical pump/x-ray probe technique has been used to study photophysical and photochemical molecular processes.[10–13] An all-x-ray pump-probe experiment with attosecond x-ray pulses has been proposed in Ref. 8. The pump pulse interacts with the system to create a valence-excited state wave packet which evolves for a controlled delay time τ when a second probe pulse interacts with it. τ is not limited by the core-hole lifetime. The dependence of this coherent stimulated x-ray Raman signal (CXRS) on the delay time τ carries information about valence-excited state dynamics. The pump-probe signal may be recast in the doorway/window representation of optical nonlinear spectroscopy.[14] In Ref. 8 these were computed within the equivalent core single Slater determinant approximation. Here we express them using the single-body Green's functions (GF), thus avoiding the explicit computation of the many-electron core excitations.

The Green's functions have been extensively used to study x-ray absorption fine structure (XAFS).[15–20] The formalism is well developed and incorporates intrinsic and extrinsic losses[19] coming from the many-body interactions (electron-phonon, electron-hole pairs, etc.). These provide a high level, yet practical, approach that goes beyond the density-functional theory considered in Ref. 8. By invoking the "sudden approximation" whereby a core hole is created and destroyed instantaneously, we express the signal in terms of the one-particle Green's functions which parametrically depend on the core hole.[19]

We compare CXRS with resonance inelastic x-ray Raman scattering (RIXS) which is a common frequency-domain technique used in the study of core-excited states in solids and molecules.[21–24] The RIXS signal can be described by the Kramers-Heisenberg expression,[23,25] as done for valence excitations in the optical regime,[14]

$$S_{\mathrm{RIXS}}(\omega_1,\omega_2)=\sum_{ac}|A_{ca}(\omega_1)|^2\delta(\omega_1-\omega_2-\omega_{ca}), \tag{1}$$

with the transition amplitude

$$A_{ca}(\omega_1)=\sum_e \frac{B_{ce}B_{ea}}{\omega_1-\omega_{ea}+i\Gamma_{ea}}, \tag{2}$$

where ω_1 and ω_2 are the incoming and scattered photon frequencies, a and c denote the valence N-electron ground state and singly-excited states, and e is the excited state with one core hole and $N+1$ valence electrons. B_{ea} and B_{ce} are matrix elements of dipole operator.

Displaying this signal vs $\omega_1-\omega_2$ reveals the valence transitions (ω_{ca}). The core-hole resonances ω_{ea} in the transition amplitude A_{ca} are typically much broader and less resolved due to the large core-hole lifetime contribution to Γ_{ea} which is $\sim$0.05 eV.[25] CXRS is a closely related technique performed with a pair of attosecond pulses. We show how the signal can be recast in a form resembling Eq. (1), making it a natural time-domain extension of RIXS. Varying the envelopes of both pulses and their delay offer a much higher degree of control of the signal. Both signals can be described as a valence electron-hole wave packet (a doorway state) prepared by the pump beam with high spatial and temporal resolution. This wave packet is probed by projecting it into a second (window) wave packet prepared by the probe.[26] This wave packet can be visualized in real space when the valence excitations are treated at the configuration-interaction single (CIS) level.

Equation (1) can be derived in the time domain using the closed-time path loop (CTPL) diagram shown in Fig. 1. This diagram may then be modified to represent CXRS. In this diagram time runs clockwise and all the interactions are ordered along the loop. In physical time, however, only interactions on the same branch of the loop are time ordered with respect to each other. Interactions on different branches are not time ordered.[27] The correlation-function expression for the RIXS signal is readily obtained from Fig. 1 by assigning each interaction an excitation operator (B or $B^\dagger$) according to the rules given in Ref. 27. We then get

$$S_{\mathrm{RIXS}}(\omega_1,\omega_2,t)=2\,\mathrm{Re}\int_{-\infty}^{\infty}ds_2\int_0^{\infty}ds_1\int_0^{\infty}ds_3 e^{-i\omega_2 s_2}e^{i\omega_1(s_1+s_2+s_3)}$$
$$\times E_1(t-s_1-s_2)E_1^*(t-s_3)$$
$$\times\langle B_m(t-s_3)B_m^\dagger(t)B_n(t-s_2)B_n^\dagger(t-s_1-s_2)\rangle. \tag{3}$$

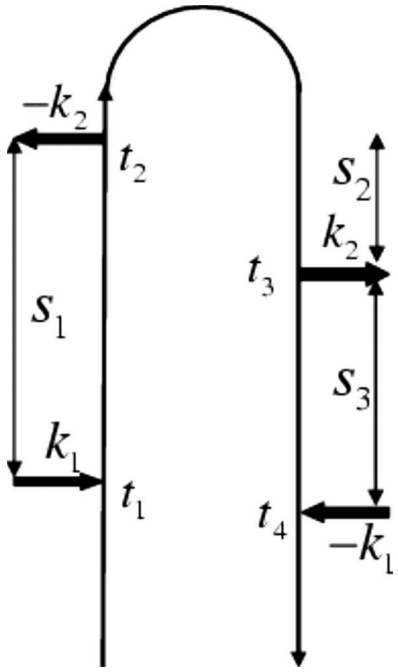

FIG. 1. CTPL diagram representing the RIXS [Eq. (3)]. Time runs on the loop clockwise starting from bottom of the left strand. Interactions on each branch are time ordered with respect to each other. Interactions in different branches are not time ordered. The incoming and detected modes are denoted by the indices 1 and 2, respectively. s_1, s_2, and s_3 are positive time intervals along the loop. By ordering the interactions in different branches, Fig. 1 can be decomposed into three diagrams corresponding to three different Liouville space pathways (Ref. 14). However, this will not be necessary here.

The operator $B_m^\dagger(B_m)$ creates (annihilates) a core-hole/valence-electron pair,

$$B_m = \sum_i \mu_{im} c_i c_m^\dagger, \quad B_m^\dagger = \sum_i \mu_{mi} c_m c_i^\dagger. \tag{4}$$

Here c_m annihilates electron at the mth core orbital and $c_i^\dagger$ creates an electron at the ith valence orbital. These are Fock space Fermi operators. ω_1 and ω_2 are the carrier frequencies of the two pulses and μ_{im} is the dipole matrix element between the ith valence orbital and nth core orbital. $E_j(\mathbf{r},t)$, $j=1,2$ are complex field envelopes,

$$E_j(\mathbf{r},t) = E_j e^{ik_j\cdot\mathbf{r}-i\omega_j t} + E_j^* e^{-ik_j\cdot\mathbf{r}+i\omega_j t}. \tag{5}$$

The time dependence of exciton operators in Eq. (3) is given by the free molecular Hamiltonian (no field), $B_m(t) = e^{iHt}B_m e^{-iHt}$. By inserting the identity operator $\Sigma_\nu|\nu\rangle\langle\nu|$, expanded in the many-body states of the molecule, between the exciton operators in the middle of Eq. (3) and assuming stationary field $E_j(t)=1$, we can carry out the s_2 integration and we immediately recover the Kramers-Heisenberg (KH) expression (1) for the signal.

The single-particle many-body Green's functions provide a standard tool for computing x-ray absorption near-edge spectra (XANES).[19] Computer codes based on the GW approximation (where vertex corrections are ignored) developed for these Green's functions are broadly applied to molecules and crystals.[15–18] We next show that the signal can be approximately expressed in terms of these Green's functions. The correlation function in Eq. (3) can be recast as

$$\begin{aligned}&\langle B_m(t-s_3)B_m^\dagger(t)B_n(t-s_2)B_n^\dagger(t-s_1-s_2)\rangle \\ &\quad = \langle a|B_m U(-s_3)B_m^\dagger U(s_2)B_n U(s_1)B_n^\dagger|a\rangle,\end{aligned} \tag{6}$$

where $|a\rangle$ is the ground many-body state with N valence electrons. $U(s)=e^{iHs}$ is the time evolution operator and H is free molecular Hamiltonian. We set the ground-state energy $\omega_a=0$.

We next define the following projection operator in the $N+1$ valence electron/1 core-hole space:

$$\mathcal{P}_m = \sum_i c_i^\dagger c_m |a\rangle\langle a| c_m^\dagger c_i. \tag{7}$$

$\mathcal{P}_m$ selects a subspace of the full $N+1$ electron space which includes single valence electron-hole pair excitations. By inserting the projection operator (7) twice inside the average on the right-hand side of Eq. (6), we obtain an approximate expression for the correlation function. Using Eqs. (4) and (7), it factorizes into a product of three correlation functions,

$$\begin{aligned}&\langle B_m(t-s_3)B_m^\dagger(t)B_n(t-s_2)B_n^\dagger(t-s_1-s_2)\rangle \\ &\quad \approx \langle a|B_m U(-s_3)\mathcal{P}_m B_m^\dagger U(s_2)B_n \mathcal{P}_n U(s_1)B_n^\dagger|a\rangle \\ &\quad = \sum_{ijkl}\sum_{i'j'} \mu_{im}\mu_{mk}\mu_{jn}\mu_{nl}\langle a|c_m^\dagger c_i U(-s_3)c_{i'}^\dagger c_m|a\rangle \\ &\quad \times \langle a|c_{i'}c_k^\dagger U(s_2)c_j c_{j'}^\dagger|a\rangle\langle a|c_n^\dagger c_{j'}U(s_1)c_l^\dagger c_n|a\rangle.\end{aligned} \tag{8}$$

Since the core holes are highly localized on the parent atom, their dynamics is very slow compared to the valence electrons and may be ignored. We shall ignore this dynamics and treat the core-hole indices as fixed parameters.

We next introduce the following set of many-body states:

$$|\chi(i,j)\rangle = c_i c_j^\dagger|a\rangle. \tag{9}$$

These represent one electron-hole pair excitation state of the valence N-electron system with one electron-hole pair.

We define the one-electron Green's function computed in the presence of a core hole at m,

$$G_{ij}^{(m)}(t,t') = -i\langle Tc_i(t)c_j^\dagger(t')\rangle_m, \tag{10}$$

where T is the time-ordering operator which rearranges a product of operators in increasing order in time from the right to the left and $\langle\cdot\rangle_m$ represents a trace over N-electron ground state of the valence in the presence of Coulomb potential due to a core hole at m.

We also define the one-sided Fourier transform

$$G_{j'l}^{R(n)}(\omega_1) = \int_0^\infty dt\, e^{-i\omega_1 t}G_{j'l}^{(n)}(t), \tag{11}$$

where G^R is the retarded Green's functions.[28]

Using Eqs. (9) and (10), the correlation function (8) can be recast as

$$\langle B_m(t-s_3)B_m^\dagger(t)B_n(t-s_2)B_n^\dagger(t-s_1-s_2)\rangle$$
$$= \sum_{ijkl}\sum_{i'j'} \mu_{im}\mu_{mk}\mu_{jn}\mu_{nl}\theta(s_1)\theta(s_3)G_{i'i}^{(m)\dagger}(s_3)G_{j'l}^{(n)}(s_1)$$
$$\times\langle\chi(i',k)|e^{-iHs_2}|\chi(j,j')\rangle. \quad (12)$$

The many-body eigenstates $|c\rangle$ (with energy $\epsilon_c=\omega_{ac}$) of the molecular Hamiltonian H at the CIS level are given by the linear combinations of single electron-hole pair states,

$$|c\rangle = \sum_{ij} f_{c;ij}|\chi(i,j)\rangle, \quad (13)$$

where $f_{c;ij}$ are expansion coefficients. $|c\rangle$ constitute an orthonormal single electron-hole pair basis set,

$$\sum_c |c\rangle\langle c| = \sum_{ij} |\chi(i,j)\rangle\langle\chi(i,j)| = 1. \quad (14)$$

Inserting this identity into the last term in Eq. (12) and substituting it in Eq. (3) gives

$$S_{\mathrm{RIXS}}(\omega_1,\omega_2) = -\sum_{ijkl}\sum_{i'j'}\sum_{mnc} f_{c;i'k}f_{c;j'j}^*\mu_{im}\mu_{mk}\mu_{jn}\mu_{nl}$$
$$\times\int_0^\infty ds_1\int_0^\infty ds_3\theta(s_1)\theta(s_3)e^{i\omega_1(s_1+s_3)}$$
$$\times\int_{-\infty}^\infty ds_2 e^{i(\omega_1-\omega_2-\omega_{ac})s_2}E_1(t-s_1-s_2)$$
$$\times E_1^*(t-s_3)G_{ii'}^{(m)\dagger}(s_3)G_{j'l}^{(n)}(s_1), \quad (15)$$

where $\omega_{ac}=\omega_a-\omega_c$. Equation (15) corresponds to the RIXS signal obtained earlier using the Keldysh Green's functions[29] approach [Eq. 47 in Ref. 30]. However unlike in Ref. 30, the RIXS signal derived here takes into account the shape of incoming pulse which provides a better control on the signal.

Assuming stationary field envelopes, the s_2 integral in Eq. (15) reduces to a Dirac-delta function and Eq. (15) takes the KH form (1) with the transition amplitude

$$A_{ca}(\omega_1) = \sum_{nljj'} f_{c;jj'}G_{j'l}^{R(n)}(\omega_1)\mu_{jn}\mu_{nl}. \quad (16)$$

Equation (16) may be interpreted as follows. The N-electron ground state $|a\rangle$ is excited by the incoming x-ray beam, creating a core-excited state with $(N+1)$ valence electrons. This state evolves during the short-time window permitted by the core-hole lifetime. This evolution in the presence of a core hole is described by the frequency-dependent Green's function. Finally this excited state is transformed by a dipole transition to a singly-excited valence ground state $|c\rangle$.

II. X-RAY PUMP-PROBE SIMULATED RAMAN SIGNAL

We assume high probe intensity so that stimulated emission is dominant and spontaneous emission can be neglected. The signal is given by the difference between the transmitted intensities of the probe (k_2) with and without the pump (k_1). Four CTPL diagrams contribute to the signal for our two-band model (Fig. 2).

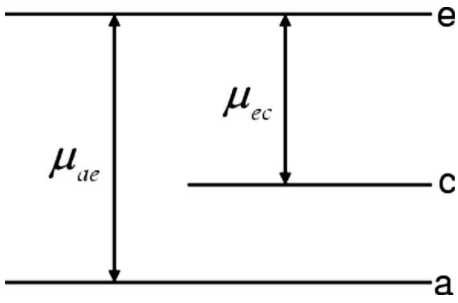

FIG. 2. Three-level sequential transition dipole scheme used for pump-probe signal. a and c are valence ground and excited states, and e is the valence $(N+1)$-electron excited state in the presence of one core hole.

When the pump and probe pulse envelopes are well separated in time, the process may be separated into three steps. First, two interactions with the pump create a wave packet of electron-hole pair states $|c\rangle$ in the valence N-electron system. This wave packet evolves during the delay τ and modulates the absorption of the probe. The two loop diagrams shown in Figs. 3(a) and 3(b) contribute to the signal. These diagrams represent two different correlation functions of the exciton operators. Details are given in Appendix A. The signal can be expressed in the doorway/window form,[6,8,14]

$$S_{\mathrm{CXRS}}(\tau) = \sum_{ac}[D_{ac}W_{ca}e^{-i\omega_{ac}\tau} + \mathrm{c.c.}], \quad (17)$$

where c.c. represents the complex conjugate. The pump prepares a doorway wave packet (A6),

$$|D\rangle = \sum_c D_{ac}|c\rangle, \quad (18)$$

and the probe creates a window wave packet (A7),

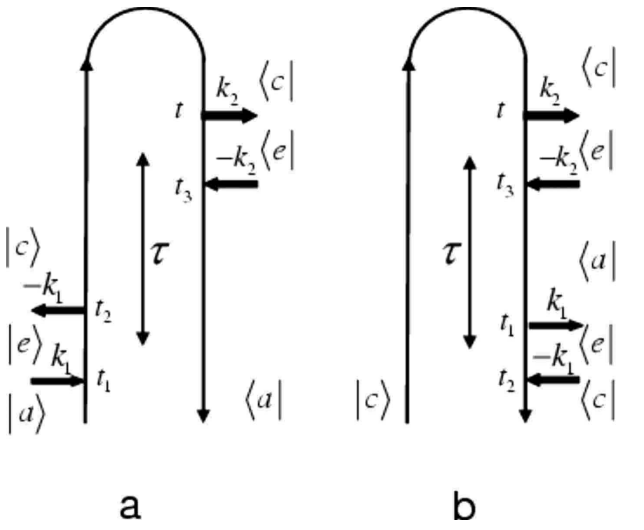

FIG. 3. Two CTPL diagrams that contribute to the pump-probe signal for a two-valence-level scheme sketched in Fig. 2.

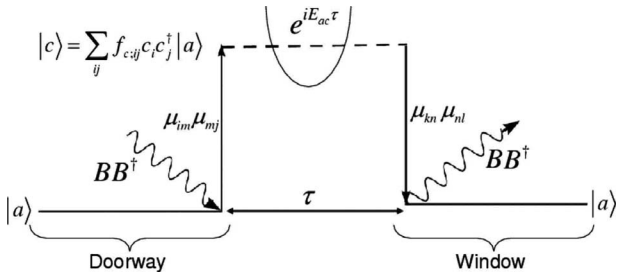

FIG. 4. Schematic of doorway and window in Eqs. (21) and (22).

$$|W\rangle = \sum_c W_{ac}|c\rangle. \tag{19}$$

The signal is given by the overlap of these wave packets. Note that the signal in Eq. (17) is given for $\tau > 0$ (pump interacts before the probe pulse). However, in order to express the CXRS signal in a form similar to RIXS (21), for $\tau < 0$, we define the CXRS signal to be the same as in Eq. (17).

Fourier transform of Eq. (17) gives

$$S_{\mathrm{CXRS}}(\omega) = \sum_{ac} D_{ac} W_{ca} \delta(\omega - \omega_{ca}) + \sum_{ac} [D_{ac} W_{ca}]^* \delta(\omega + \omega_{ca}). \tag{20}$$

As was done in Eq. (16) for RIXS, we can express the doorway and the window in terms of the Green's functions and the CIS coefficients. Details are given in Appendix B. We then obtain

$$D_{ac} := P(a) \sum_{ijk} \mu_{im}\mu_{mj} f^*_{c;ik} \int \frac{d\omega}{2\pi} G^{R(m)}_{kj}(\omega - \omega_{ca}) \times E_1^*(\omega) E_1(\omega - \omega_{ca}), \tag{21}$$

$$W_{ca} := 2 \sum_{ijk} \mu_{kn}\mu_{nj} f_{c;ji} \int \frac{d\omega}{2\pi} \mathrm{Im}\{G^{R(n)}_{ki}(\omega - \omega_{ca})\} \times E_2(\omega) E_2^*(\omega - \omega_{ca}). \tag{22}$$

Note that the exact expression for the pump-probe signal, Eq. (15) with Eqs. (A6) and (A7), requires the computation of many-body states for the N and the $N+1$ valence-electron systems. In contrast, the Green's function expressions, Eqs. (21) and (22), only require the one-particle Green's functions and valence-excited states at the CIS level. These may be obtained using standard electronic structure computer codes. In Appendix C we show that Eqs. (A6) and (A7) reduce to Eqs. (21) and (22) within the CIS approximation.

The physical picture offered by the doorway and the window in Eqs. (21) and (22) is shown schematically in Fig. 4. The system interacts twice with the pump creating a valence-excited state electronic wave packet [Eq. (18) together with Eq. (21)]. This wave packet evolves freely for a time τ, which is not limited by the core-hole lifetime. The two dipole matrix elements μ_{im} and μ_{mj} represent the two interactions with the x-ray pulse which create and annihilate the core hole at m. The Green's function $G_{kj}(\omega)$ together with coefficients $f^* c; ik$ represents the relevant dynamics. The window, Eq. (19) with Eq. (22), is similarly created by the probe x-ray pulse and the signal is given by the overlap of these two wave packets.

III. CONCLUSIONS

We have presented the many-body Green's function theory of stimulated attosecond Raman x-ray scattering. The Green's function expression avoids the explicit computation of the ground and the core-hole excited states of the system. The single-particle Green's functions can be obtained by the self-consistent solution of Hedin's equations[31–33] which is implemented in standard computer codes.[19] We have assumed that the core hole is localized and only enters as a parameter. This allows one to express the signal using the single-particle Green's functions. The "shakeup" and "shake-off" excitations,[19] in which more than one electron is excited due to the creation of a core hole, is included within the CIS approximation. Equation (12) expresses the correlation function of exciton operators in terms of the single-electron Green's functions and the particle-hole propagator for valence orbitals. The propagator is subsequently expressed in terms of the CIS expansion coefficients for the valence-excited states. This approximation can be relaxed by calculating this propagator using the time-dependent Hartree-Fock (TDHF). Since TDHF is often insufficient, higher-order corrections can be derived systematically using the many-body expansion for the particle-hole propagator.[34] The present formulation can be extended to incorporate core-hole and nuclear dynamics through the corresponding Green's functions using equation of motion technique[35] as was done in Ref. 30.

ACKNOWLEDGMENTS

The support of the Chemical Sciences, Geosciences and Biosciences Division, Office of Basic Energy Sciences, Office of Science, U.S. Department of Energy is gratefully acknowledged. We thank Igor Schweigert for useful scientific comments.

APPENDIX A: DERIVATION OF EQ. (17)

The correlation-function expression corresponding to the diagrams shown in Figs. 3(a) and 3(b) is given by

$$S_{\mathrm{CXRS}}(\tau) = 2\,\mathrm{Re} \int_{-\infty}^{\infty} dt \int_{-\infty}^{t} dt_3 \left[\int_{-\infty}^{\infty} dt_2 \int_{-\infty}^{t_2} dt_1 \langle B(t_3) B^\dagger(t) \times B(t_2) B^\dagger(t_1) \rangle + \int_{-\infty}^{\infty} dt_1 \int_{-\infty}^{t_1} dt_2 \langle B(t_2) B^\dagger(t_1) \times B(t_3) B^\dagger(t) \rangle \right] E_1^*(t_2 - \tau) E_1(t_1 - \tau) E_2(t) E_2^*(t_3). \tag{A1}$$

Since the pulses are temporally well separated and are short compared to the time delay τ, the upper limits of t_2 and t_3

integrals in the first and second terms may be safely extended to infinity. Interchanging the integration variables t_1 and t_2 in the first term we obtain

$$S_{\mathrm{CXRS}}(\tau) = 2\,\mathrm{Re}\int_{-\infty}^{\infty} dt \int_{-\infty}^{t} dt_3 \int_{-\infty}^{\infty} dt_1 \int_{-\infty}^{t_1} dt_2 E_2(t) E_2^*(t_3) \times [\langle B(t_3)B^\dagger(t)B(t_1)B^\dagger(t_2)\rangle E_1^*(t_1-\tau)E_1(t_2-\tau) + \langle B(t_2)B^\dagger(t_1)B(t_3)B^\dagger(t)\rangle E_1^*(t_2-\tau)E_1(t_1-\tau)]. \tag{A2}$$

The correlation functions in Eq. (A2) can be expanded in terms of the many-body states of the system. By inserting the identity operator $I=\Sigma_\nu|\nu\rangle\langle\nu|$, where $\nu=c,e$, we obtain

$$\langle B(t_3)B^\dagger(t)B(t_1)B^\dagger(t_2)\rangle = \sum_{acee'} P(a)B_{ae}B_{ec}^\dagger B_{ce'}B_{e'a}^\dagger e^{i\omega_{ec}t}e^{-i\omega_{ea}t_3}e^{i\omega_{e'a}t_2}e^{-i\omega_{e'c}t_1}, \tag{A3}$$

where $B_{ac}=\langle a|B|c\rangle$, etc., and $P(a)$ is the equilibrium probability of the system to be in state $|a\rangle$. A similar expression can be obtained for the other correlation function. Substituting these results in Eq. (A2) and defining the Fourier transform of the pulse envelope as

$$E(t) = \int \frac{d\omega}{2\pi} e^{i\omega t}E(\omega), \tag{A4}$$

the signal can be expressed in the doorway/window representation as[68,14]

$$S_{\mathrm{CXRS}}(\tau) = \sum_{ac}[D_{ac}W_{ca}e^{-i\omega_{ac}\tau} + \mathrm{c.c.}], \tag{A5}$$

where the doorway wave packet is given by Eq. (18) with

$$D_{ac} = \sum_e P(a)B_{ae}B_{ec}^\dagger \int \frac{d\omega}{2\pi}\frac{E_1(\omega)E_1^*(\omega+\omega_{ac})}{\omega+\omega_{ec}+i\eta}. \tag{A6}$$

The window wave packet is similarly given by Eq. (19) with

$$W_{ca} = \sum_e B_{ce}B_{ea}^\dagger \int \frac{d\omega}{2\pi}\left[\frac{1}{\omega+\omega_{ec}+i\eta} - \frac{1}{\omega+\omega_{ec}-i\eta}\right]E_2(\omega)E_2^*(\omega+\omega_{ac}). \tag{A7}$$

Since in the limit $\eta\to 0$,

$$\frac{1}{\omega+\omega_{ec}\pm i\eta} = \mathrm{PP}\frac{1}{\omega+\omega_{ec}} \mp i\pi\delta(\omega+\omega_{ec}), \tag{A8}$$

where $\mathrm{PP}(1/x)$ denotes the principal part of $1/x$, the frequency integration in Eq. (A7) can be performed, resulting in

$$W_{ca} = 2\pi\sum_e B_{ce}B_{ea}^\dagger E_2(\omega_{ce})E_2^*(\omega_{ac}). \tag{A9}$$

APPENDIX B: THE GREEN'S FUNCTION EXPRESSION FOR THE PUMP-PROBE SIGNAL

We start with Eq. (A1) and allow for the creation of a core hole at m and n. The interaction with E_1 (E_1^*) [$E_2(E_2^*)$] creates (destroys) a core hole at m [n]. We then have

$$S_{\mathrm{CXRS}}(\tau) = 2\,\mathrm{Re}\int_{-\infty}^{\infty} dt \int_{-\infty}^{t} dt_3 \left\{ \int_{-\infty}^{\infty} dt_2 \int_{-\infty}^{t_2} dt_1 \langle B_n(t_3)B_n^\dagger(t)B_m(t_2)B_m^\dagger(t_1)\rangle + \int_{-\infty}^{\infty} dt_1 \int_{-\infty}^{t_1} dt_2 \langle B_m(t_2)B_m^\dagger(t_1)B_n(t_3)B_n^\dagger(t)\rangle \right\} E_1^*(t_2-\tau)E_1(t_1-\tau)E_2(t)E_2^*(t_3). \tag{B1}$$

Inserting the projection operators twice in Eq. (4), the correlation function in the first term can be expressed as

$$\langle B_n(t_3)B_n^\dagger(t)B_m(t_2)B_m^\dagger(t_1)\rangle \approx \sum_a P(a)\langle a|B_n(t_3)\mathcal{P}_nB_n^\dagger(t)B_m(t_2)\mathcal{P}_mB_m^\dagger(t_1)|a\rangle = \sum_a P(a)\sum_{ijkl}\mu_{im}\mu_{mj}\mu_{kn}\mu_{nl}e^{i\omega_a(t_3-t_1)}\langle a|c_kc_n^\dagger U(t_3-t)\mathcal{P}_nc_nc_l^\dagger U(t-t_2)c_ic_m^\dagger\mathcal{P}_mU(t_2-t_1)c_mc_j^\dagger|a\rangle. \tag{B2}$$

Substituting this back in Eq. (B1), and changing variables $t_2-t_1=s'$ and $t-t_3=s$, the first term can be expressed as

$$I_1 = 2\,\mathrm{Re}\sum_a P(a)\sum_{ijkl}\mu_{im}\mu_{mj}\mu_{kn}\mu_{nl}\int_{-\infty}^{\infty} dt\int_0^{\infty} ds\int_{-\infty}^{\infty} dt_2\int_0^{\infty} ds' e^{i\omega_a(t-t_2)} \times G_{ki'}^{(n)\dagger}(s)G_{j'j}^{(m)}(s')\langle\chi(i',l)|U(t-t_2)|\chi(i,j')\rangle E_2(t)E_2^*(t-s)E_1^*(t_2-\tau)E_1(t_2-s'-\tau), \tag{B3}$$

where the $|\chi(i,j)\rangle$ basis is defined in Eq. (9) and

$$\theta(s)\langle a|c_m^\dagger c_iU(s)c_j^\dagger c_m|a\rangle = i\theta(s)e^{-i\omega_{a^s}}G_{ij}^{(m)}(s),$$

$$\theta(s)\langle a|c_m^\dagger c_i U(-s)c_j^\dagger c_m|a\rangle = -i\theta(s)e^{i\omega_a s}G_{ij}^{(m)\dagger}(s). \tag{B4}$$

Inserting the identity operator in terms of the CIS states in Eq. (13), Eq. (B3) finally becomes

$$I_1 = 2\,\mathrm{Re}\sum_{ac} P(a)\sum_{ijkl}\sum_{i'j'} \mu_{im}\mu_{mj}\mu_{kn}\mu_{nl}f_{c;li'}f_{c;ij'}^* \int_{-\infty}^{\infty} dt \int_0^{\infty} ds e^{-i\omega_{ca}t}G_{ki'}^{(n)\dagger}(s)E_2(t)E_2^*(t-s)$$
$$\times \int_{-\infty}^{\infty} dt_2 \int_0^{\infty} ds' e^{i\omega_{ca}t_2}G_{j'j}^{(m)}(s')E_1^*(t_2-\tau)E_1(t_2-s'-\tau). \tag{B5}$$

Performing Fourier transform [Eq. (A4)], Eq. (B3) can also be expressed as

$$I_1 = 2\,\mathrm{Re}\sum_{ac} P(a)\sum_{ijkl}\sum_{i'j'} \mu_{im}\mu_{mj}\mu_{kn}\mu_{nl}f_{c;li'}f_{c;ij'}^* \int \frac{d\omega}{2\pi} G_{ki'}^{R(n)\dagger}(\omega-\omega_{ca})E_2(\omega)E_2^*(\omega-\omega_{ca})e^{i\omega_{ca}\tau}$$
$$\times \int \frac{d\omega'}{2\pi} G_{j'j}^{R(m)}(\omega-\omega_{ca})E_1^*(\omega)E_1(\omega-\omega_{ca}), \tag{B6}$$

where $G_{ij}^{R(m)}(\omega)$ is defined in Eq. (11).

Proceeding along the same steps that lead from Eq. (B2) to Eq. (B6) and taking the complex conjugate (this is allowed since we are looking for the real part), the second term in Eq. (B1) can be recast as

$$I_2 = -2\,\mathrm{Re}\sum_{ac} P(a)\sum_{ijkl}\sum_{i'j'} \mu_{im}\mu_{mj}\mu_{kn}\mu_{nl}f_{c;lj'}f_{c;ii'}^* \int \frac{d\omega}{2\pi} G_{kj'}^{R(n)\dagger}(\omega-\omega_{ca})E_2(\omega)E_2^*(\omega-\omega_{ca})e^{i\omega_{ca}\tau}$$
$$\times \int \frac{d\omega'}{2\pi} G_{i'j}^{R(m)\dagger}(\omega-\omega_{ca})E_1^*(\omega)E_1(\omega-\omega_{ca}). \tag{B7}$$

The signal is finally given by

$$S_{\mathrm{CXRS}}(\tau) = I_1 + I_2, \tag{B8}$$

which results in Eqs. (21) and (22).

APPENDIX C: EQUIVALENCE OF EQS. (A6) AND (A7) AND EQS. (21) AND (22) WITHIN THE CIS APPROXIMATION

The pump-probe signal is given by Eq. (15) where the doorway and the window are given in terms of the many-body states by Eqs. (A6) and (A7). The Green's function expressions are given by Eqs. (21) and (22).

We first expand the GF in the many-body states. Using Eqs. (11) and (B4), we can write

$$G_{ij}^{R(m)}(\omega+\omega_{ac}) = -i\int_0^{\infty} dt e^{-i(\omega-\omega_c)t}\langle a|c_m^\dagger c_i U(t)c_j^\dagger c_m|a\rangle. \tag{C1}$$

By inserting the identity operator, $\Sigma_e|e\rangle\langle e|$, before and after the evolution operator and performing the integration over time, Eq. (C1) reduces to

$$G_{ij}^{R(m)}(\omega+\omega_{ac}) = -\sum_e \frac{\langle a|c_i c_m^\dagger|e\rangle\langle e|c_m c_j^\dagger|a\rangle}{\omega+\omega_{ec}-i\eta}. \tag{C2}$$

Substituting this in Eqs. (21) and (22), we obtain

$$D_{ac} := -\sum_{ijke} P(a)\mu_{im}\mu_{mj}f_{c;ik}^*\langle a|c_k c_m^\dagger|e\rangle \times\langle e|c_m c_j^\dagger|a\rangle \int \frac{d\omega}{2\pi}\frac{E_1^*(\omega)E_1(\omega-\omega_{ca})}{\omega+\omega_{ec}-i\eta}, \tag{C3}$$

$$W_{ca} := -\sum_{ijke} \mu_{kn}\mu_{nj}f_{c;ji}\langle a|c_i c_n^\dagger|e\rangle \times\langle e|c_n c_k^\dagger|a\rangle \int \frac{d\omega}{2\pi}\left[\frac{1}{\omega+\omega_{ec}+i\eta} - \frac{1}{\omega+\omega_{ec}-i\eta}\right] E_2(\omega)E_2^*(\omega-\omega_{ca}). \tag{C4}$$

We next consider the expressions for the doorway and window in terms of the many-body states. Using Eq. (4), Eqs. (A6) and (A7) can be expressed as

$$D_{ac} = \sum_{ije} P(a)\mu_{im}\mu_{mj}\langle a|c_i c_m^\dagger|e\rangle \times\langle e|c_m c_j^\dagger|c\rangle \int \frac{d\omega}{2\pi}\frac{E_1(\omega)E_1^*(\omega+\omega_{ac})}{\omega+\omega_{ec}+i\eta} \tag{C5}$$

and

$$W_{ca} = \sum_{ije} \mu_{kn}\mu_{nj}\langle c|c_k c_n^\dagger|e\rangle\langle e|c_n c_j^\dagger|a\rangle \int \frac{d\omega}{2\pi}\left[\frac{1}{\omega+\omega_{ec}+i\eta} - \frac{1}{\omega+\omega_{ec}-i\eta}\right]E_2(\omega)E_2^*(\omega+\omega_{ac}). \quad \text{(C6)}$$

Using the CIS expansion for the excited states $|c\rangle$, Eq. (13), we can write

$$\langle e|c_m c_j^\dagger|c\rangle = \sum_{i'j'} f_{c;i'j'}\langle e|c_m c_j^\dagger c_{i'} c_{j'}^\dagger|a\rangle = \sum_{j'} f_{c;jj'}\langle e|c_m c_{j'}^\dagger|a\rangle, \quad \text{(C7)}$$

where in going to the second line the sum over i' can be done since state $|e\rangle$ corresponds to single excited $N+1$ valence electrons. Substituting Eq. (C7) in Eq. (C5) we get

$$D_{ac} = \sum_{ijke} P(a)\mu_{im}\mu_{mj} f_{c;jk}\langle a|c_i c_m^\dagger|e\rangle \times\langle e|c_m c_k^\dagger|a\rangle \int \frac{d\omega}{2\pi}\frac{E_1(\omega)E_1^*(\omega+\omega_{ac})}{\omega+\omega_{ec}+i\eta}. \quad \text{(C8)}$$

Taking the complex conjugate and interchanging dummy indices i and j, Eq. (C8) becomes the same as Eq. (C3). Similarly one can show that Eq. (C6) is the same as Eq. (C4) within CIS approximation. This proves the equivalence of Eqs. (A6) and (A7) and Eqs. (21) and (22).

[1] M. Drescher, M. Hentschel, R. Kienbereger, G. Tempea, C. Spielman, G. A. Reider, P. B. Corkum, and F. Krausz, Science **291**, 1923 (2001).
[2] R. F. Service, Science **298**, 1356 (2002).
[3] Reviews on *Attosecond Spectroscopy* in the special issue of Science 317 (2007).
[4] I. Thomann, E. Gregonis, X. Liu, R. Trebino, A. S. Sandhu, M. M. Murnane, and H. C. Kapteyn, Phys. Rev. A **78**, 011806(R) (2008); L. Miaja-Avila, G. Saathoff, S. Mathias, J. Yin, C. La-o-vorakiat, M. Bauer, M. Aeschlimann, M. M. Murnane, and H. C. Kapteyn, Phys. Rev. Lett. **101**, 046101 (2008).
[5] F. Dorchies, F. Blasco, C. Bonte, T. Caillaud, C. Fourment, and O. Peyrusse, Phys. Rev. Lett. **100**, 205002 (2008).
[6] S. Mukamel, Phys. Rev. B **72**, 235110 (2005).
[7] V. Felicissimo, F. Guimaraes, F. Gel'mukhanov, A. Cesar, and H. Agren, J. Chem. Phys. **122**, 094319 (2005).
[8] I. V. Schweigert and S. Mukamel, Phys. Rev. A **76**, 012504 (2007).
[9] S. Tanaka and S. Mukamel, Phys. Rev. Lett. **89**, 043001 (2002).
[10] C. Bressler and M. Chergui, Chem. Rev. (Washington, D.C.) **104**, 1781 (2004).
[11] D. A. Oulianov, I. V. Tomov, A. S. Dvornikov, and P. M. Rentzepis, Proc. Natl. Acad. Sci. U.S.A. **99**, 12556 (2002).
[12] L. X. Chen, X. Zhang, E. C. Wasinger, K. Attenkofer, G. Jennings, A. Z. Muresan, and J. S. Lindsey, J. Am. Chem. Soc. **129**, 9616 (2007); L. X. Chen, Annu. Rev. Phys. Chem. **56**, 221 (2005).
[13] R. Santra, C. Buth, E. R. Peterson, R. W. Dunford, E. P. Kanter, B. Krassig, S. H. Southworth, and L. Young, J. Phys.: Conf. Ser. **88**, 012052 (2007).
[14] S. Mukamel, *Principles of Nonlinear Optical Spectroscopy* (Oxford University Press, New York, 1995).
[15] C. A. Ashley and S. Doniach, Phys. Rev. B **11**, 1279 (1975).
[16] J. J. Rehr and A. L. Ankudinov, Coord. Chem. Rev. **249**, 131 (2005).
[17] J. A. Soininen, A. L. Ankudinov, and J. J. Rehr, Phys. Rev. B **72**, 045136 (2005).
[18] A. L. Ankudinov, B. Ravel, J. J. Rehr, and S. D. Conradson, Phys. Rev. B **58**, 7565 (1998).
[19] J. J. Rehr and R. C. Albers, Rev. Mod. Phys. **72**, 621 (2000).
[20] Yejun Feng, J. A. Soininen, A. L. Ankudinov, J. O. Cross, G. T. Seidler, A. T. Macrander, J. J. Rehr, and E. L. Shirley, Phys. Rev. B **77**, 165202 (2008).
[21] F. Gel'mukhanov and H. Ågren, Phys. Rep. **312**, 87 (1999).
[22] M. Magnuson, L.-C. Duda, S. M. Butorin, P. Kuiper, and J. Nordgren, Phys. Rev. B **74**, 172409 (2006); C. Sathe, F. F. Guimaraes, J.-E. Rubensson, J. Nordgren, A. Agui, J. Guo, U. Ekstrom, P. Norman, F. Gel'mukhanov, and H. Ågren, Phys. Rev. A **74**, 062512 (2006).
[23] F. de Groot and A. Kotani, *Core Level Spectroscopy of Solids* (CRC/Taylor & Francis, New York, 2008); A. Kotani and S. Shin, Rev. Mod. Phys. **73**, 203 (2001).
[24] H. Sternemann, J. A. Soininen, C. Sternemann, K. Hamalainen, and M. Tolan, Phys. Rev. B **75**, 075118 (2007); S. Galambosi, M. Knaapila, J. A. Soininen, K. Nygard, S. Huotari, F. Galbrecht, U. Scherf, A. P. Monkman, and K. Hamalaineen, Macromolecules **39**, 9261 (2006).
[25] Y. Hikosaka, Y. Velkov, E. Shigemasa, T. Kaneyasu, Y. Tamenori, J. Liu, and F. Gel'mukhanov, Phys. Rev. Lett. **101**, 073001 (2008).
[26] L. E. Fried and S. Mukamel, J. Chem. Phys. **93**, 3063 (1990).
[27] C. Marx, U. Harbola, and S. Mukamel, Phys. Rev. A **77**, 022110 (2008).
[28] A. Fetter and J. D. Walecka, *Quantum Theory of Many-Particle Systems* (Dover, New York, 2003).
[29] H. Haug and A.-P. Jauho, *Quantum Kinetics in Transport and Optics of Semiconductors* (Springer-Verlag, Berlin, 1996).
[30] T. Privalov, F. Gel'mukhanov, and H. Ågren, Phys. Rev. B **64**, 165116 (2001).
[31] L. Hedin, Phys. Rev. **139**, A796 (1965).
[32] F. Aryasetiawan and O. Gunnarsson, Rep. Prog. Phys. **61**, 237 (1998).
[33] G. Onida, L. Reining, and A. Rubio, Rev. Mod. Phys. **74**, 601 (2002).
[34] J. Lindenberg and Y. Őhrn, *Propagators in Quantum Chemistry*, 2nd ed. (Wiley, New Jersey, 2004).
[35] D. C. Langreth, Phys. Rev. **182**, 973 (1969).